Organic Design of Biomorphic Superstructures

Huynh, Tan-Phat

Published in:
CHEMSYSTEMSCHEM

DOI:
10.1002/syst.202000031

Published: 01/09/2020

Document Version
Accepted author manuscript

Document License
Publisher rights policy

Organic design of biomorphic superstructures

Dr. Tan-Phat Huynh

Laboratory of Molecular Science and Engineering, Åbo Akademi University, Porthaninkatu 3-5, 20500 Turku, Finland

E-mail: tan.huynh@abo.fi

Abstract

Nature has endowed extraordinary beauty and functional significance in the form of biological morphology. Inspired by nature, biomorphic superstructures have been designed and synthesized from organic precursors in a laboratory. While the complexity of synthetic superstructures is dim compared to natural forms, from an engineering point of view they possess competitive advantages such as low cost, ease of fabrication, and, occasionally, unexpected characteristics. Thus, there are still plenty of exciting biomorphic superstructures awaiting to be discovered.

Keywords: biomorphic, self-assembly, superstructures, crystallization, lamellar

1. Introduction

The term “biomorphic abstraction” is popularized in the book “*Cubism and Abstract Art*”, written by Alfred H. Barr in 1936.[1] The “biomorphic” in art has been connected to forms or shapes of living creatures, where the possible “biomorphs” are flowers, plant shapes, and protozoans.[2] Therefore, the design process inspired by the biomorphic shapes and patterns refers, to some extent, the term “biomorphism”. Figure 1a shows images of the elaborately mineral exoskeleton of marine microfossils, exemplifying delicate and intricate natural biomorphs.[3] In materials design and technology, the emerging biomorphic structures not only mimic the organic morphology but also capture the functions of a biological model. The materials with the biomorphic structures on micro and meso scales, namely biomorphic superstructures, are the focus of interest in this minireview.

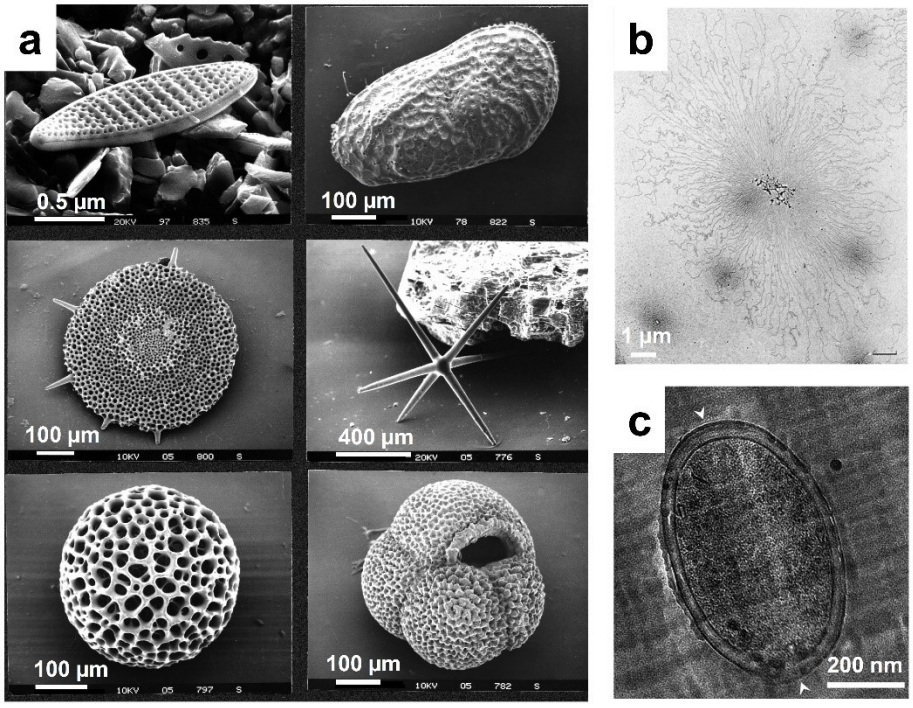

Figure 1. Biological superstructures: scanning electron microscopy (SEM) images of (a) the marine microfossils: (from left-to-right then top-to-bottom) diatom, ostracod, radiolaria I, sponge spicule, radiolaria II, planktonic foraminifera (Photo credit: Hannes Grobe) and (b) the

deoxyribonucleic acid (DNA) supercoils released when chromosomes from *Escherichia coli* are in the hypophases containing 0.4 M salt (Reproduced with permission from [4]); (c) A cryo-electron micrograph of the cross section of a *Mycobacterium smegmatis* cell deformed by the cutting process.[5]

Since the natural biomorphs are the direct inspiration for this review, it is worth recalling the mechanism, the self-assembly in particular, behind the evolution of biomorphs.[6] In this process, all the information required to assemble the biomolecules is encoded into their sequence in the form of amino acids, nucleobases, etc. so that they are ready to perform intermolecular interactions. Readers are therefore encouraged to gain preliminary knowledge in molecular and supramolecular interactions involved in the self-assembly, which can be found in other literature.[7] From a thermodynamic point of view, the correct self-assembly represents the optimized structure of the biomorphic assemblies of the lowest Gibb's free energy. However, some self-assembled chiral materials has been found to possess two or more ground states (two or more local minima), and a slight bias, i.e. one state is favored than the other, is observed.[8]

There is a plethora of examples in the self-assembly of natural biomorphs ranging from short biomolecules like phospholipids and peptides to hundred nm-size viruses. In the scope of introducing the biological superstructures, examples of typical μm-scale biomaterials are presented. Deoxyribonucleic acid (DNA), mentioned in any biology textbook, forms a double-helix structure from the self-assembly of two polynucleotide chains. The process is driven by the stacking of the amine bases and the multiple hydrogen bonds formed between pairs of nucleobases, i.e. the adenine-thymine and guanine-cytosine.[9] While the length of this helical structure is in the nm-scale, the DNA is able to form highly organized tertiary structures – the supercoils.[4, 10] The length of the supercoils is up to mm but able to fit inside the cell. Upon being triggered, the supercoils of hundred μm (Figure 1b) released from the cell. The tertiary structures are also assembled from other biological matters such as proteins, e.g. the human insulin[11] and

the bovine pancreatic ribonuclease[12]. Different from the bovine pancreatic ribonuclease, the individual polypeptide chains of insulin do not contain the information for self-assembly, i.e. insulin is synthesized from a larger precursor, namely preproinsulin, instead. The process is therefore categorized as “self-assembly with post-modification”.[6b, 13] Additionally, the self-assembly of proteins is a key to superstructure formation of viruses such as tobacco mosaic virus, M13 bacteriophage, and rotavirus.[14] The assembled superstructure of the M13 bacteriophages is of interest as it has been used as template for several biomorphic superstructures presented in this review.[15] Their general superstructures consist of a circular, single-stranded DNA genome encased in a tube-like self-assembled proteins. Not only did the DNAs and proteins use in the self-assembly of natural biomorphs but also the phospholipids. For instance, the cell membrane of *M. smegmatis* up to micrometer scale in diameter as shown in Figure 1c,[5] is self-assembled from phospholipid bilayers. In the environment of biological fluids, the hydrophilic heads turn outward to the surrounding medium (e.g. via hydrogen bonding and dipolar interactions) while the hydrophobic tails repelled water molecules and interact with each other through vdW force.[16] The organization of the phospholipids using multiple weak bonding motifs keeps the membrane intact.

Self-assembly of biomolecules into hierarchical superstructures can be also found in daily-life bio-based products, given the silk and carrageenan gel.[17] The former one is constituted from fibroin – a protein found in the storage sac of the female *Nephila clavata*. The morphological evolution continues with the self-assembly of fibroin into the granule-based microfibrils. Subsequently, the microfibrils an hierarchical structure of dragline fibers up to µm-scale long.[17a] The gelation of carrageenan, on the other hand, hypothetically includes two steps: (i) formation of double-helix domains and (ii) domain crosslinking by cations through ion-ion interactions.[17b] Many more examples of natural biomorphs that can be found in other reports.[18] It is worth mentioning that due to the structure-oriented feature of the biomorphs, their applications are extensively exploited, especially in biomineralization.[19] This includes the development of hybrid

materials using a template approach, or in other words, modification of ubiquitously biological templates with synthetic materials.[20]

This minireview offers an alternative approach for biomorphism. Herein we will discuss in-depth principles used to design and synthesize biomorphic superstructures in a *non-templated* self-assembly from organic molecules or macromolecules precursors. These principles open the door for the creation of novel biomorphic superstructures with exciting morphologies, properties, and functionalities. Thus, the minireviews aim is to provide the reader with current reports on synthetic superstructures and associate them with the aforementioned biological forms.

2. Organic design of biomorphic superstructures

This section is highlighting a minor group of nature-mimicked or biomorphic superstructures synthesized from organic (macro)molecules, namely the organic design of the biomorphic superstructures. The synthetic process is primarily non-templated self-assembly of the molecules (section 2.1) and macromolecules (section 2.2) as two main sources from which the biomorphic superstructures are evolved.

2.1 Molecular approach

Crystallization process, where the molecules are packed into highly organized structures, has been used to produce mm-size organic crystals.[21] Notably, crystallization of the biomorphic superstructures from organic molecules is remarkable and happens either inside a solution[22] or at a water-air interface[23]. For example, crystallization of DL-alanine in a particular condition creates partly hollow tubes of mm in length and μm in width.[22] The morphology of the tube is highly pH-dependent, e.g. shorter and thinner tubes are obtained at basic conditions (pH between 8 and 10). These square-shaped tubes resemble hollow structure of the kapok fiber[24], even though the interior of the tube still accommodates partly disordered nanoparticulate building blocks. The microtube-like superstructure was also reported by Pampalakis et al.[25], in which a

complex of oleic acid with iron has also been used. This superstructure is named an organic Fe(III) oleate garden since it is inspired by the concept of a chemical garden (or chemobrionic)[26]. Instead of growing upwards from a crystal seed like traditional gardens, this tube is grown inversely from isopropanol solution. This process includes two steps which the cm-sized Fe(III) oleate precipitates (i) dislodging to the surface of the solution and (ii) growing downwardly by gravity. However, the growth was unsuccessful in non-polar solvent like toluene since the $FeCl_3$ crystal was unable to be solvated.

To obtain hierarchical superstructures with higher complexity, molecular design must be considered. For instance, a designed fullerene (C60) derivative (Figure 2a) can be self-organized into an hierarchical superstructure of a flower shape (Figure 2b, 2e-h, and 2i).[27] These flower-like biomorphs are self-assembled from the disk-shaped pedals engaging in the π-π and vdW interactions of C60 moieties and aliphatic chains, respectively. These supramolecular interactions were confirmed by using fast Fourier transform (FFT) analysis, i.e. revealing the distance of the lamellar bilayers at the edge of the flower which matches the molecular length of the bearing alkyl chains of the C60 derivative. In addition, the self-assembly of the C60 derivative in the chiral butanol solvents generates left- and right-handed spiral superstructures (Figure 2c and 2d).

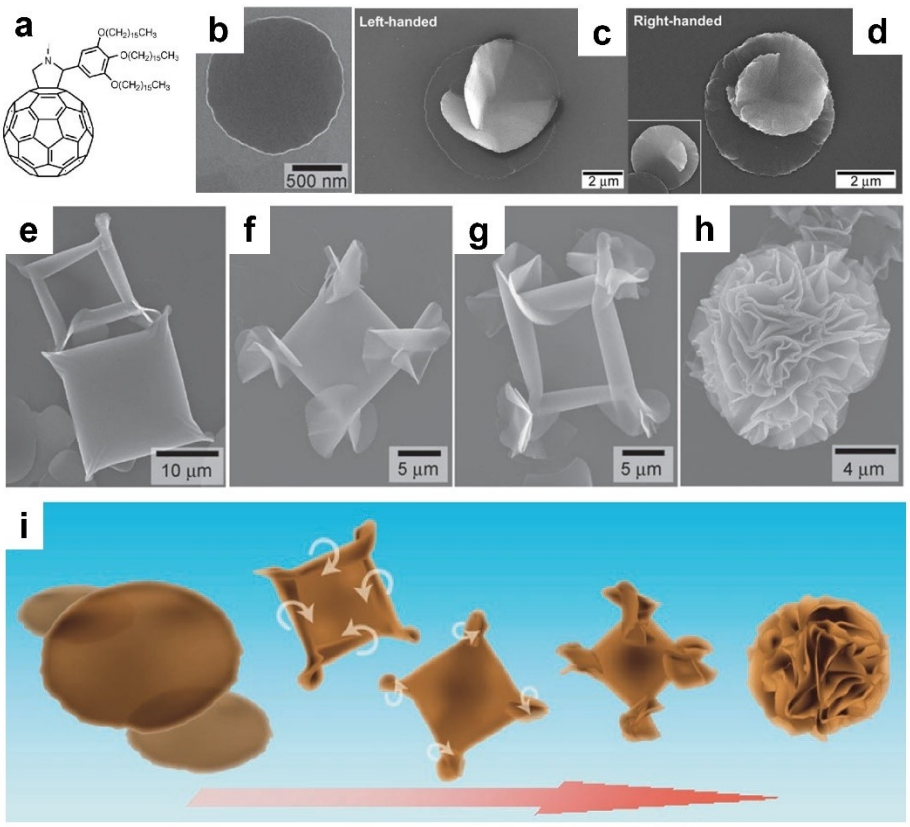

Figure 2. (a) Structural formula of the C60 derivative; SEM images of (b) the disk-shaped assemblies formed in 1,4-dioxane at 20 °C, (c) right-handed and (d) left-handed spiral assemblies obtained in 2-(*R*)-butanol and 2-(*S*)-butanol, respectively, (e) the square-shaped objects loosely rolled up in every corner formed by rapid cooling of the solution from 60 °C to 5 °C, (f and g) the further rolled-up objects of crumpled structures at the four corners, (h) the final flower-shaped objects formed by slow aging at 58 °C. (i) Schematic illustration explains the formation of the flower-like superstructure. (Reproduced with permission from [27])

Resuming our discussion on the flower-like superstructures, the work of Martin et al.[28] with porphyrin, a macrocycles known to form H- and J-aggregates[28-29], must be described. Figure 3a show molecular formulas of anionic and cationic porphyrins which have been used to assemble the four-leaf clover-shaped superstructures (Figure 3b). The metal centers of the porphyrin are either electron donors or electron acceptors depending on the complexed metals, e.g. Zn or Sn,

respectively. Nevertheless, the intermolecular interactions arising from the metals in the porphyrin play only a minor role in self-assembly, i.e. the clover-like superstructures are produced even with free-base porphyrins. This conclusion is further supported by the work of During et al.[29c] on the biomorphic microneedles grown from ionic free-base porphyrins. While the clover morphology transforms as the ionic strength and temperature of the self-assembly reaction vary, the structures still maintain a 4-fold symmetry. The temperature exhibited more pronounced influence on morphology of the self-assemblies (Figure 3b) than the that of ionic strength. The study also pointed out the potential to tune functionality (such as the electronic and photophysical properties) of these materials by altering the metals in the porphyrins and/or varying the cooperative interactions between the porphyrin subunits. The tunable properties raise the possibility of fabricating, for example, semiconducting materials. This viewpoint is demonstrated in the work of Liu et al.[30], i.e. modification of the side chains of the (porphinato)Zn(II) building blocks lead to diverse redox potentials of the biomorphic superstructures. Not only did the authors tune the electrochemical potentials, but also they generate different biomorphic shapes including 2-D nanosheets, nanowires, fibers and amorphous solids.

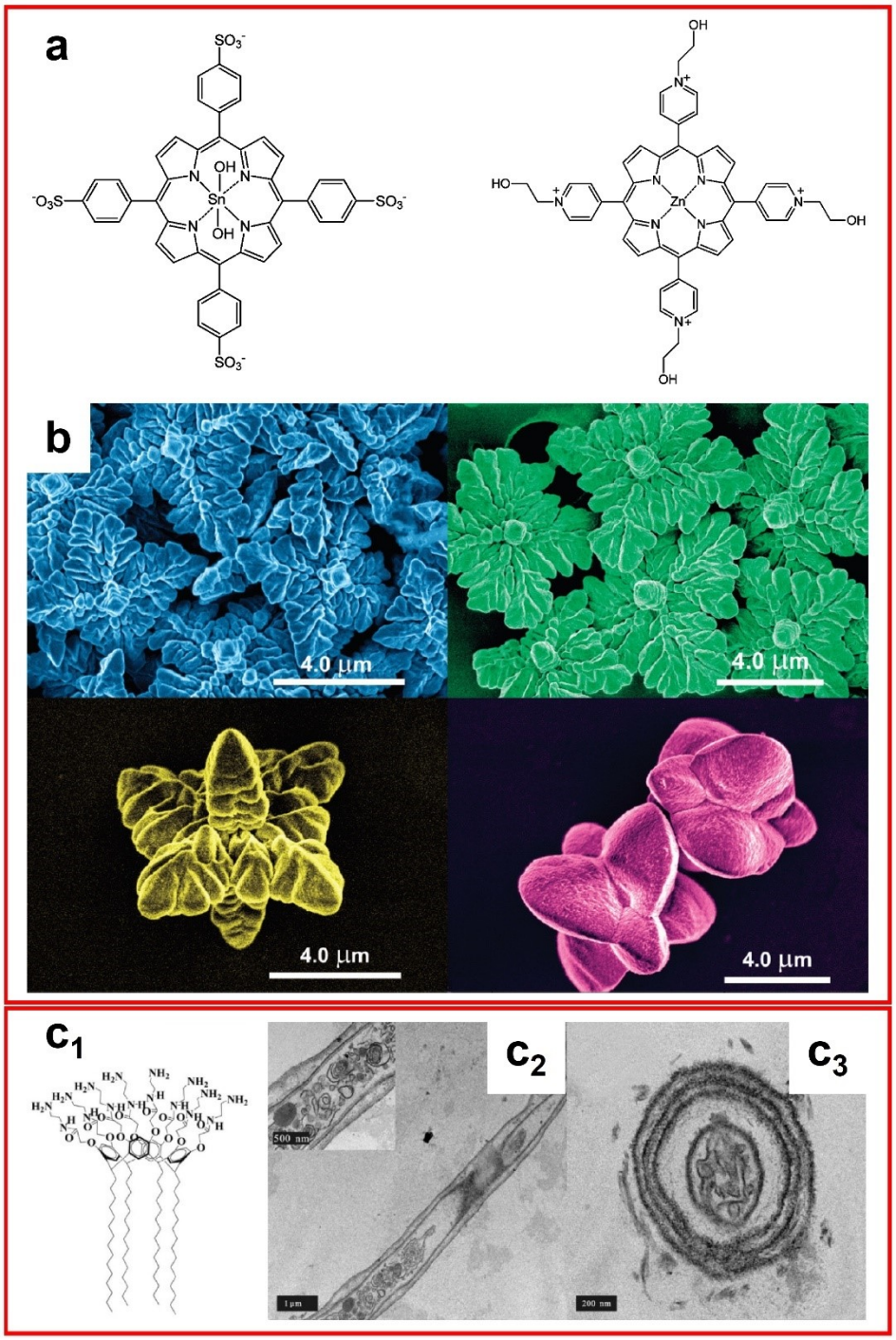

Figure 3. (a) Chemical formulas of the anionic (left) and cationic (right) porphyrins of different metal centers; (b) SEM images of the clover-like superstructures grown at 10 (blue), 23 (green), 60 (gold), and 80 °C (pink). (Reproduced with permission from [28]) (c_1) The molecular structure of the amphiphilic aminoresorcinarene, transmission electron microscopy (TEM) images of the (c_2)

profile section with a magnified inset and (c_3) cross section of the microtube. The nanoparticle (NP) aggregates are encapsulated inside the tube. The microtubes were prepared by incubating the aminoresorcinarene solution of 150 μM at room temperature for 1 month. (Reproduced with permission from [31])

Solvent polarity (or dipole moment) also causes dramatic changes in resulting biomorphic superstructures; therefore, the solvent effect in self-assembly of the macrocycles was investigated.[32] Interference of solvent molecules with the supramolecular assemblies was observed in study of 2,3,9,10,16,17,24,25-octakis(phenoxy)phthalocyaninato zinc (Zn[Pc($OPh)_8$]) molecules. On the one hand, the self-assembled Zn[Pc($OPh)_8$] superstructures possess the nanobelts in n-hexane, but soft nano-sticks or microscale needle mushrooms as well as pine leaves (depending on aggregation time) in methanol on the other hand. Additionally, other macrocycles like the aminoresorcinarenes (Figure $3c_1$) are able to form microtubes using a straightforward mixing process. The mechanism lies on the amphiphilicity of the protonated aminoresorcinarenes in water that drives the system to the formation of aggregated microtubes.[33] Furthermore, the microtubes can be decorated externally or internally with various metal NPs through coordination or electrostatic interaction of protonated amine of the aminoresorcinarenes and metal NPs (Figure $3c_2$ and $3c_3$).[31] These hybrid materials possess new interesting properties such as uptake and release of given NPs.

2.2 Macromolecular approach

In a similar way of molecular approaches (discussed in section 2.1), macromolecules undergo self-assembly and result biomorphic superstructures. Besides, solutions of macromolecules, e.g. in water, possesses high viscosity so that they are printable. Next paragraph demonstrates a process of printing biomorphic superstructures from solutions of macromolecules.

2.2.1 Approach from biopolymers and biohybrid materials

The superstructures can be derived from single- or multi-component self-assembly of biomolecules such as peptide amphiphiles[34]. Two macroscopic superstructures, namely sacs and torus, have been reported. In both cases, the self-assembly is simply driven by the electrostatic interactions between positively charged peptides and negatively charged biomacromolecules at a liquid/liquid interface (Figure 4a). This leads the formation of a diffusion barrier, which helps to prevent chaotic mixing, upon contact between the two liquids. Owning shorter diffusion path and a higher surface area/volume ratio compared to the sacs, the toroidal gel (Figure 4b-d) fabricated by Hedegaard et al.[34b] is of great interest. The torus is a product of co-assembly of the peptide amphiphiles with a range of extracellular matrix proteins and biomolecules including fibronectin, collagen, keratin, elastin-like proteins, and hyaluronic acid. The gel has been printed under cell diluent environment (Figure 4) where the size and ring-shape of the microgels has been guided by the nozzle diameter and shear forces during the bioprinting process, respectively.

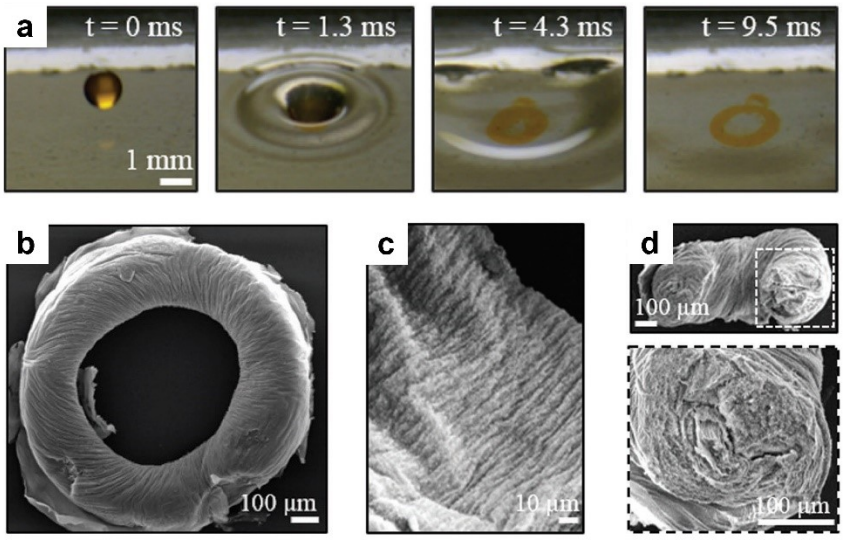

Figure 4. (a) Formation of the toroidal gel when a droplet of peptide amphiphiles of 10 mg mL^{-1} is injected into the keratin solution of 20 mg mL^{-1} using 500-µm nozzle; SEM images of (b) a

toroidal gel of ~500 μm in diameter, (c) surface and (d) cross-section of a toroidal gel (Reproduced with permission from [34b]).

Self-assembly into chiral supramolecules includes, but not limited to, superstructures derived from the insulin[35], organo-soluble peptide-poly(n-butyl acrylate)[36], colloidal particles of the M13 bacteriophage[37], (bacterial nanocellulose)-alginate macro-fiber[38]. These helical superstructures have been employed in many interesting applications including effective substrate for surface-enhanced Raman spectroscopy (SERS),[35] chiral reflector/filters,[37] electrical generator,[39] and materials of high strength and toughness[38]. In all cases, the chirality of the hybrid materials is guided either by the biomaterials, e.g. M13 bacteriophage, or by switching macromolecules to chiral forms using pH[36]. Figure 5 illustrates the self-templating process of M13 phages of which the superstructures are affected by two critical factors, i.e. the local induction of chiral liquid-crystal phase transitions and the interfacial forces at the meniscus. Depending on arrangement of the M13 phages, three superstructures including nematic orthogonal twist, cholesteric helical ribbon, and smectic helicoidal nanofilament, have been grown. Among these superstructures, the smectic nanofilaments exhibited capability of generating piezoelectric energy. Their power performance is structure-dependent, i.e. the device power fabricated from the micro-patterns of 2D-phage-dot is ~40 times higher than that from the continuous phage thin-film.[39]

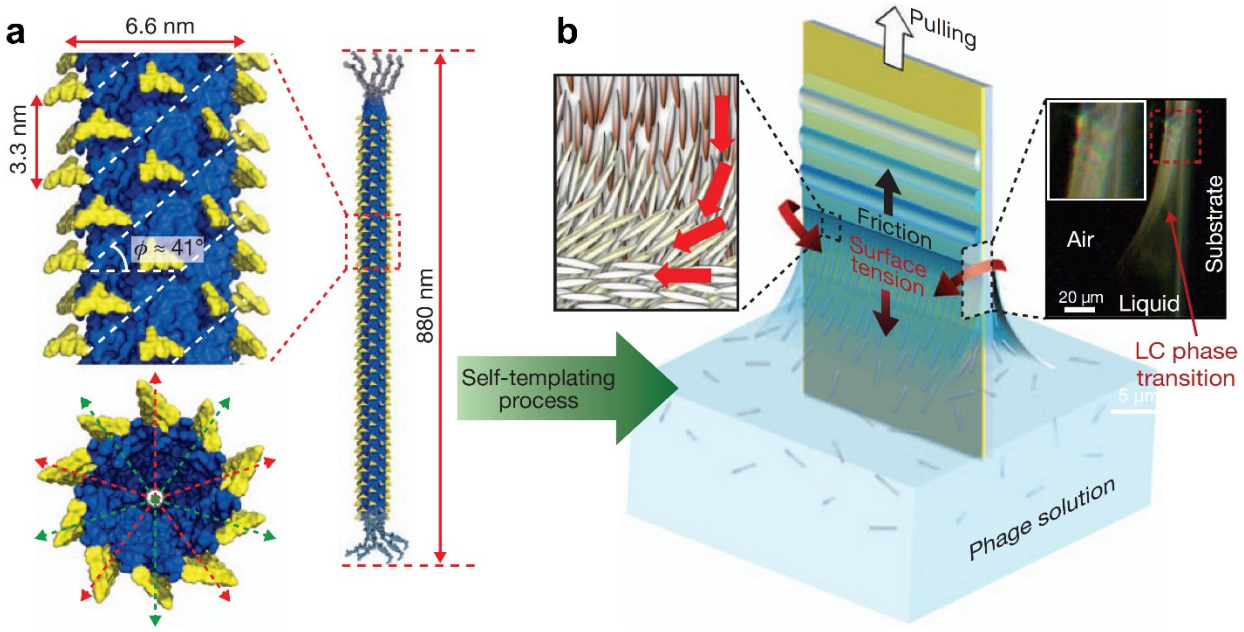

Figure 5. Schematic diagram of the phage-based self-templating process. (a) Schematic illustrations of the phage structure with a helical angle (ϕ) of 41° with periodic subunit spacing of 3.3 nm and (b) of the helical self-templating assembly of phage particles controlled by competing interfacial forces at the meniscus where liquid crystal phase transitions occur. The polarized optical microscopy image shows iridescent colors originating from liquid crystal phase formation at the air–liquid–solid interface. (Reproduced with permission from[37])

Section 2.1 has briefly mentioned the biomorphic tubes synthesized from the Fe(III) oleate chemical gardens. In the effort of providing a closer look into the link of chemical gardens with the origins of life, the gel/liquid interface approach has been utilized in sprouting calcium phosphates[40] – the minerals found many living organisms. A profound work is from Punia et al.[41] which demonstrated the growth of a sponge-like gelatin-intercalated calcium phosphate tubules. By varying the percentages (0−15 w/v%) of the gelatin, the tube diameters can be tuned from 200 μm to 2 mm. These superstructures greatly serve as life-supporting scaffolds, evidenced by the attachment and healthy growth of individual cells (marine (*Pyrocystis lunula*) and mammalian

(HeLa and H9C2) cell lines) to form multicellular entities. Similar organic-inorganic intercalation has been also observed in the nacre architecture, which often illustrated as a “brick-and-mortar” arrangement.[42] The “brick” herein is highly aligned inorganic aragonite platelets that is surrounded by the “mortar” – a protein matrix. Inspired by this, a nacre-mimicked superstructures is synthesized by vacuum filtration or water evaporation of the chitosan-montmorillonite hybrid building blocks.[43] The architecture of the nano-laminar organization is self-assembly induced which results fire-retardant property. Thus, the superstructure exhibits the potential application as heat-resistant and gas-barrier materials. Not only biopolymers but also synthetic polymers are used to synthesize lamellar superstructures that are presented in the next section.

2.2.2 Approach from synthetic polymers

In the end of section 2.2.1, laminated superstructures have mimicked structures of chemical gardens and nacre. This section will continue with lamellar superstructures assembled from synthetic polymers such as polyimide, (ether ketone)-based polymers, and poly(acrylic acid).[44] A group of (ether ketone)-based polymers has generated spindle- and platelet-like superstructures through crystallization.[44a, 44d] Their morphologies vary with the synthetic conditions such as types of solvents, temperature and time. The first example is the hierarchically lamellar platelet-like superstructure was assembled from poly(ether ether ketone) (PEEK) when the gelation of PEEK (following with freeze-drying) carried out in 4-chlorophenol instead of dichloroacetic acid.[44d] This is attributed to the π-π interactions between PEEK and 4-chlorophenol facilitating slower growth, thus developing more ordered crystalline lamella. Under a particular condition such as mixture of water and tetrahydrofuran (THF), the lamellae of amphiphilic diblock copolymers can reorganize to the onion-like vesicles of which ~13 nm is the distance between layers.[44c] The self-assembly is attributed to the aggregation of the polymers since the hydrophobic blocks became insoluble when water was added. With more than one superstructures found, the reversible transformation between superstructures could be observed

for the diblock copolymers in the solvent mixtures, i.e. poly(ferrocenyldimethylsilane)-block-polyisoprene in THF/decane[45] and polystyrene-block-poly(D-lactide acid) in THF/water[46]. Both copolymers form fiber-like structures at high ration of THF but transform to caterpillar-like[45] and torus-like[46] superstructures when the ratio of THF is lower. Figure 6 shows the caterpillar-like superstructure (also observed in amphiphilic triblock co-micelles[47]) formed upon the addition of THF solution of the polymers into THF/decane mixture, but reversed to fiber-like structure when THF is evaporated. It is worth mentioning that the caterpillar-like superstructure (Figure 6, left image), which is scarce, is successfully grown under low nucleation in the presence of large amounts of polar solvent (here is THF).

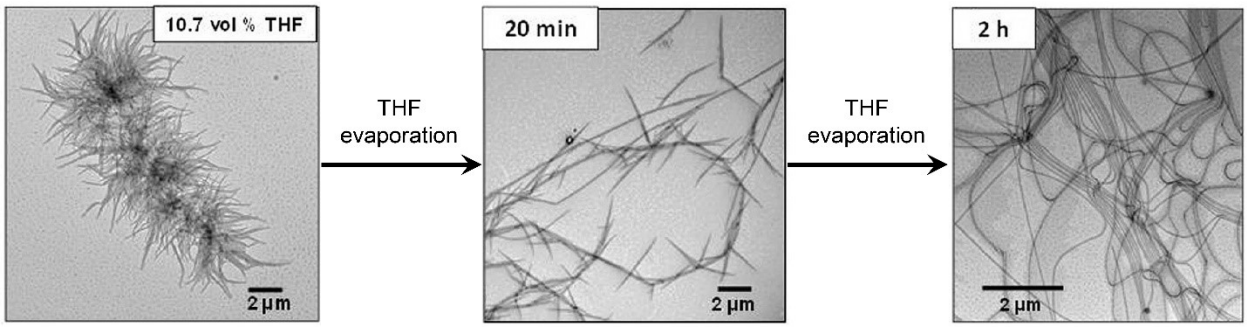

Figure 6. TEM images demonstrate transformation of the caterpillar-like superstructure formed from diblock copolymers in a THF/decane mixture to the fiber-like structure upon the removal of THF by mild rotary evaporation. (Reproduced with permission from [45])

The effect of polar solvent was also utilized for engineering other biomorphic superstructures. For instance, self-assembly of biodegradable poly(ethylene glycol)-block-poly(D,L-lactide) polymers to the (red blood cell – RBC)-like stomatocytes requires up to 50 v% water at a rate of 1 mL h^{-1} under vigorous stirring condition.[48] Since RBCs are highly important in medical treatment of the circulation system as well as low oxygen-level diseases, the biomorphic stomatocytes are potentially used as alternatives if oxygen-releasing function is

provided. Indeed, hemoglobin and the photosensitizer chlorin e6 are encapsulated inside the stomatocytes.[48a] Furthermore, stomatocytes are covered with an erythrocyte-derived cell membrane so that the physicochemical properties of the superstructures matched those of RBCs. However, the stomatocytes (~0.5 μm) have not yet mimicked the size of RBCs (~30 μm), i.e. two order-of-magnitude lower. The effect of water is also seen in development of spiral superstructures.[49] Here water-oil emulsion droplets are used as soft templates to create a controllable microenvironment for preparation of chiral superstructures. The chirality of the superstructures can be induced by doping polyaniline (PANI) with enantiomeric r- or s-camphorsulfonic acids.[49a] On the other example, chiral particles (Figure 7) synthesized by direct emulsification of polypeptides including α-helical homo- and copolypeptides of γ-benzyl glutamate and allylglycine, produce spiral superstructures (Figure 7a).[49b] The chirality of the spirals was controlled by the chirality of the α-helices. The mechanism of the sprial superstructures is not yet fully been understood, but it is hypothesized that the spirals observed in the present study are the result of folded fibril bundles of coiled helical polypeptides (Figure 7b).

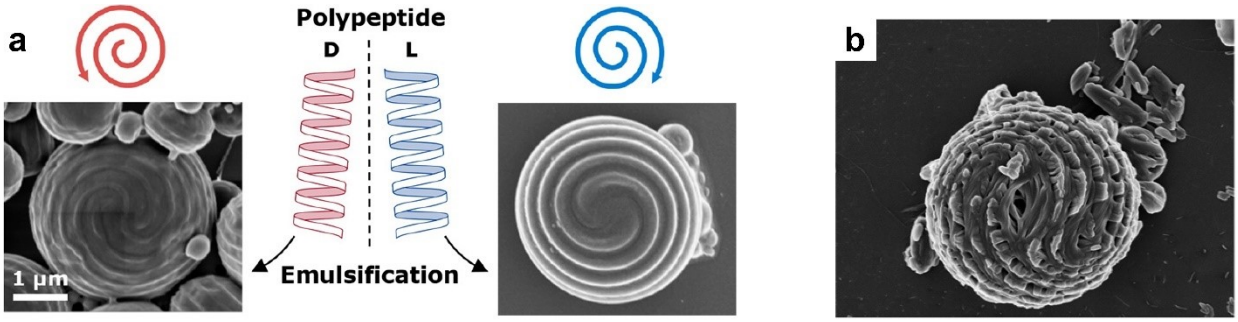

Figure 7. (a) Schematic illustrations of the right-handed α-helical polypeptides (rich in L residues) produced clockwise spirals, whereas left-handed α-helical polypeptides (rich in D residues) produced the enantiomorphs, i.e., counterclockwise spirals. SEM images are of the (a) spiral superstructures and (b) particle with fiberous features, prepared from polypeptide-toluene solution in water emulsions. (Reproduced with permission from [49b])

The term “self-assembly with post-modification” has been introduced, “precursor modification followed by self-assembly”, in contrast, implys that the starting materials undergo a chemical transformation prior to self-assembly. Several approaches have been used to trigger the precursor modification, an interesting one is redox modification. At the molecular level, redox coordinates the water-soluble perylene diimide molecules to engage in π-π stacking interaction and thus promotes self-assembly into superstructures.[50] At macromolecular level, the modification is achieved via a controlled chemical oxidation process, for example, the *o*-phenylenediamine was oxidized by ferric sulfate to form the poly(*o*-phenylenediamine)/Fe_2O_3 composites.[51] The process then resulted rose-like hierarchical microstructures which are self-assembled from several tens of thin petals with a thickness of tens of nm.

Conclusion

Having read the main text of this minireview, the readers may ask “Why do we need to study organic design of the biomorphic superstructures?”. There are several answers to this question: First, the biomorphic superstructures are developed from low-cost and ease-of-scale-up synthetic precursors compared to biomolecules. Second, the study introduces new superstructures which have not yet appeared in the life forms; thus, new knowledge emerges. This knowledge gain is not only interesting on its own, but may also benefit modern technology, i.e. engineers equip with biomorphic materials as alternatives when extraction or synthesis of the natural biomorphs is out of the reach. Last but not least, the author has suggested that design of the hybrid structures helps to impart or tune material’s properties including chiral optics, surface enhanced Raman scattering, piezoelectric enhancement, control and release of active materials. However, these opportunities also come with challenges. While there are likely many high-end products or devices to be designed which may benefit from biomorphic superstructures, only few applications of these materials have been reported. The author believes that synthetic superstructures still remain

unexplored in their early stage of low interdisciplinarity research and merits further research. A solution that came into the author's mind is exploiting the information from the use of biological templates in different fields.

Acknowledgement

T.-P.H would like to acknowledge the contribution of the European COST Action CA17120 supported by the EU Framework Programme Horizon 2020; the financial support from the starting fund from AAU's Research Profiling (Grant No. 301843), the Magnus Ehrnrooth Foundation, and the Academy of Finland (Grant No. 323240).

References

[1] A. H. Barr, *Cubism and Abstract Art*, 1st ed., Routledge, London, **1936**.

[2] a) A. Agkathidis, in *The 34th International Conference on Education and Research in Computer Aided Architectural Design* (Eds.: A. Herneoja, T. Österlund, P. Markkanen), Proceedings of eCAADe, Oulu, Finland, **2016**, pp. 291–298; b) O. Speck, D. Speck, R. Horn, J. Gantner, K. P. Sedlbauer, *Bioinspir. Biomim.* **2017**, *12*, 011004.

[3] J. Witkowski, K. Edgar, I. Harding, K. McCartney, M. Bąk, in *Encyclopedia of Marine Geosciences* (Eds.: J. Harff, M. Meschede, S. Petersen, J. Thiede), Springer Netherlands, Dordrecht, **2016**, pp. 467-475.

[4] R. Kavenoff, B. C. Bowen, *Chromosoma* **1976**, *59*, 89-101.

[5] C. Hoffmann, A. Leis, M. Niederweis, J. M. Plitzko, H. Engelhardt, *PNAS* **2008**, *105*, 3963-3967.

[6] a) M. Kirschner, T. Mitchison, *Cell* **1986**, *45*, 329-342; b) D. Philp, J. F. Stoddart, *Angewandte Chemie International Edition in English* **1996**, *35*, 1154-1196.

[7] a) G. M. Whitesides, B. Grzybowski, *Science* **2002**, *295*, 2418-2421; b) G. M. Whitesides, M. Boncheva, *PNAS* **2002**, *99*, 4769-4774; c) J. W. Steed, J. L. Atwood, *Supramolecular Chemistry*, 2nd ed., John Wiley & Sons, West Sussex, UK, **2013**; d) T.-P. Huynh, T.-A. Le, in *Molecularly Imprinted Polymers for Analytical Chemistry Applications* (Eds.: W. Kutner, P. S. Sharma), The Royal Society of Chemistry, **2018**, pp. 28-64.

[8] a) J. V. Selinger, M. S. Spector, J. M. Schnur, *J. Phys. Chem. B* **2001**, *105*, 7157-7169; b) M. S. Spector, J. V. Selinger, J. M. Schnur, in *Materials-Chirality* (Eds.: S. E. Denmark, J. Siegel, M.M. Green, R. J. M. Nolte, E. W. Meijer), Wiley-Interscience, Hoboken, New Jersey, **2004**, pp. 281-372; c) M. Wolffs, P. A. Korevaar, P. Jonkheijm, O. Henze, W. J. Feast, A. P. H. J. Schenning, E. W. Meijer, *Chem. Commun.* **2008**, 4613-4615.

[9] P. Yakovchuk, E. Protozanova, M. D. Frank-Kamenetskii, *Nucleic Acids Res.* **2006**, *34*, 564-574.

[10] S. Freeman, K. Quillin, L. Allison, M. Black, G. Podgorski, E. Taylor, J. Carmichael, *Biological Science*, 6th ed., Pearson Education, Essex, England, **2017**.

[11] J. Brange, L. Langkjœr, in *Stability and Characterization of Protein and Peptide Drugs, Vol. 5* (Eds.: W. Y.J., P. R.), Springer, Boston, MA, **1993**, pp. 315-350.
[12] G. Kartha, J. Bello, D. Harker, *Nature* **1967**, *213*, 862-865.
[13] M. Liu, M. A. Weiss, A. Arunagiri, J. Yong, N. Rege, J. Sun, L. Haataja, R. J. Kaufman, P. Arvan, *Diabetes Obes. Metab.* **2018**, *20*, 28-50.
[14] a) B. D. Harrison, T. M. A. Wilson, A. Klug, *Philos. Trans. R. Soc. London, Ser. B* **1999**, *354*, 531-535; b) S. S. Sidhu, *Biomol. Eng.* **2001**, *18*, 57-63; c) A. Charpilienne, J. Lepault, F. Rey, J. Cohen, *J. Virol.* **2002**, *76*, 7822-7831; d) S.-W. Lee, C. Mao, C. E. Flynn, A. M. Belcher, *Science* **2002**, *296*, 892-895; e) M. Young, D. Willits, M. Uchida, T. Douglas, *Annu. Rev. Phytopathol.* **2008**, *46*, 361-384; f) J. Rong, Z. Niu, L. A. Lee, Q. Wang, *Curr. Opin. Colloid Interface Sci.* **2011**, *16*, 441-450; g) R. Selvakumar, N. Seethalakshmi, P. Thavamani, R. Naidu, M. Megharaj, *RSC Adv.* **2014**, *4*, 52156-52169.
[15] P. Model, M. Russel, in *The Bacteriophages*, 2nd ed., Oxford University Press,, Plenum, New York, **2005**, pp. 375–456.
[16] K. Vogele, T. Pirzer, F. C. Simmel, *ChemSystemsChem* **2019**, *1*, e1900016.
[17] a) T.-Y. Lin, H. Masunaga, R. Sato, A. D. Malay, K. Toyooka, T. Hikima, K. Numata, *Biomacromolecules* **2017**, *18*, 1350-1355; b) E. R. Morris, D. A. Rees, G. Robinson, *J. Mol. Biol.* **1980**, *138*, 349-362.
[18] a) P. Cintas, *Angew. Chem. Int. Ed.* **2020**, *59*, 7296-7304; b) T.-P. Huynh, H. Haick, *Advanced Materials Technologies* **2019**, *4*, 1800464.
[19] a) S. Weiner, L. Addadi, *Annu. Rev. Mater. Res.* **2011**, *41*, 21-40; b) F. Nudelman, N. A. J. M. Sommerdijk, *Angew. Chem. Int. Ed.* **2012**, *51*, 6582-6596.
[20] a) J. Qian, W. Xu, W. Zhang, X. Jin, *Mater. Lett.* **2014**, *124*, 313-317; b) J. Qian, W. Xu, X. Yong, X. Jin, W. Zhang, *Mater. Sci. Eng. C* **2014**, *36*, 95-101; c) H. Ge, B. Zhao, Y. Lai, X. Hu, D. Zhang, K. Hu, *J. Mater. Sci. - Mater. Med.* **2010**, *21*, 1781-1787; d) Y. Oaki, M. Kijima, H. Imai, *J. Am. Chem. Soc.* **2011**, *133*, 8594-8599; e) M. Kijima, Y. Oaki, Y. Munekawa, H. Imai, *Chem. Eur. J.* **2013**, *19*, 2284-2293.
[21] a) I. Weissbuch, I. Kuzmenko, M. Vaida, S. Zait, L. Leiserowitz, M. Lahav, *Chem. Mater.* **1994**, *6*, 1258-1268; b) C. S. Towler, R. J. Davey, R. W. Lancaster, C. J. Price, *J. Am. Chem. Soc.* **2004**, *126*, 13347-13353.
[22] Y. Ma, H. Cölfen, M. Antonietti, *J. Phys. Chem. B* **2006**, *110*, 10822-10828.
[23] N. K. Wittig, T. E. K. Christensen, T. A. Grünewald, H. Birkedal, *ACS Materials Lett.* **2020**, *2*, 446-452.
[24] T.-T. Lim, X. Huang, *Chemosphere* **2007**, *66*, 955-963.
[25] G. Pampalakis, *Chem. Eur. J.* **2016**, *22*, 6779-6782.
[26] L. M. Barge, S. S. S. Cardoso, J. H. E. Cartwright, G. J. T. Cooper, L. Cronin, A. De Wit, I. J. Doloboff, B. Escribano, R. E. Goldstein, F. Haudin, D. E. H. Jones, A. L. Mackay, J. Maselko, J. J. Pagano, J. Pantaleone, M. J. Russell, C. I. Sainz-Díaz, O. Steinbock, D. A. Stone, Y. Tanimoto, N. L. Thomas, *Chem. Rev.* **2015**, *115*, 8652-8703.
[27] T. Nakanishi, K. Ariga, T. Michinobu, K. Yoshida, H. Takahashi, T. Teranishi, H. Möhwald, D. G. Kurth, *Small* **2007**, *3*, 2019-2023.
[28] K. E. Martin, Z. Wang, T. Busani, R. M. Garcia, Z. Chen, Y. Jiang, Y. Song, J. L. Jacobsen, T. T. Vu, N. E. Schore, B. S. Swartzentruber, C. J. Medforth, J. A. Shelnutt, *J. Am. Chem. Soc.* **2010**, *132*, 8194-8201.
[29] a) S. Mandal, S. K. Nayak, S. Mallampalli, A. Patra, *ACS Appl. Mater. Interfaces* **2014**, *6*, 130-136; b) W. Zhang, L. Xing, H. Wang, X. Liu, Y. Feng, C. Gao, *Langmuir* **2015**, *31*, 4330-4340; c) J. Düring, S. Haschke, J. Bachmann, F. Gröhn, *Colloid Polym. Sci.* **2018**, *296*, 1235-1248; d) Y. Xie, Q. Zhong, Y. Lv, J. Li, Z. Hao, C. Tang, X. Wei, Y. Su, J. Huang, A. Wang, X. Guo, J. Wang, G. Li, Y. Song, *ACS Appl. Mater. Interfaces* **2019**, *11*, 34203-34211.

[30] C. Liu, K. Liu, J. Klutke, A. Ashcraft, S. Steefel, J.-H. Olivier, *Journal of Materials Chemistry C* **2018**, *6*, 11980-11991.
[31] Y. Sun, Y. Yao, C.-G. Yan, Y. Han, M. Shen, *ACS Nano* **2010**, *4*, 2129-2141.
[32] X. Zhang, D. Gao, J. Gao, P. Zhu, M. Bouvet, Y. Chen, *RSC Adv.* **2014**, *4*, 14807-14814.
[33] Y. Sun, C.-G. Yan, Y. Yao, Y. Han, M. Shen, *Adv. Funct. Mater.* **2008**, *18*, 3981-3990.
[34] a) H.-E. Jin, J. Jang, J. Chung, H. J. Lee, E. Wang, S.-W. Lee, W.-J. Chung, *Nano Lett.* **2015**, *15*, 7138-7145; b) C. L. Hedegaard, E. C. Collin, C. Redondo-Gómez, L. T. H. Nguyen, K. W. Ng, A. A. Castrejón-Pita, J. R. Castrejón-Pita, A. Mata, *Adv. Funct. Mater.* **2018**, *28*, 1703716; c) R. M. Capito, H. S. Azevedo, Y. S. Velichko, A. Mata, S. I. Stupp, *Science* **2008**, *319*, 1812-1816.
[35] S. Wójcik, V. Babenko, W. Dzwolak, *Langmuir* **2010**, *26*, 18303-18307.
[36] J. Hentschel, H. G. Börner, *J. Am. Chem. Soc.* **2006**, *128*, 14142-14149.
[37] W.-J. Chung, J.-W. Oh, K. Kwak, B. Y. Lee, J. Meyer, E. Wang, A. Hexemer, S.-W. Lee, *Nature* **2011**, *478*, 364-368.
[38] H.-L. Gao, R. Zhao, C. Cui, Y.-B. Zhu, S.-M. Chen, Z. Pan, Y.-F. Meng, S.-M. Wen, C. Liu, H.-A. Wu, S.-H. Yu, *Nati. Sci. Rev.* **2019**, *7*, 73-83.
[39] a) B. Y. Lee, J. Zhang, C. Zueger, W.-J. Chung, S. Y. Yoo, E. Wang, J. Meyer, R. Ramesh, S.-W. Lee, *Nat. Nanotech.* **2012**, *7*, 351-356; b) K. Heo, H.-E. Jin, H. Kim, J. H. Lee, E. Wang, S.-W. Lee, *Nano Energy* **2019**, *56*, 716-723.
[40] a) K. Furuichi, Y. Oaki, H. Ichimiya, J. Komotori, H. Imai, *Sci. Technol. Adv. Mater.* **2006**, *7*, 219-225; b) M. P. Gashti, M. Stir, J. Hulliger, *Colloids Surf. B Biointerfaces* **2013**, *110*, 426-433; c) C. J. Steenbjerg Ibsen, B. F. Mikladal, U. Bjørnholt Jensen, H. Birkedal, *Chem. Eur. J.* **2014**, *20*, 16112-16120; d) E. A. B. Hughes, R. L. Williams, S. C. Cox, L. M. Grover, *Langmuir* **2017**, *33*, 2059-2067; e) E. A. B. Hughes, S. C. Cox, M. E. Cooke, O. G. Davies, R. L. Williams, T. J. Hall, L. M. Grover, *Adv. Healthcare Mater.* **2018**, *7*, 1701166.
[41] K. Punia, M. Bucaro, A. Mancuso, C. Cuttitta, A. Marsillo, A. Bykov, W. L'Amoreaux, K. S. Raja, *Langmuir* **2016**, *32*, 8748-8758.
[42] A. P. Jackson, J. F. V. Vincent, R. M. Turner, R. M. Alexander, *Proceedings of the Royal Society of London. Series B. Biological Sciences* **1988**, *234*, 415-440.
[43] a) H.-B. Yao, Z.-H. Tan, H.-Y. Fang, S.-H. Yu, *Angew. Chem. Int. Ed.* **2010**, *49*, 10127-10131; b) S.-M. Chen, H.-L. Gao, X.-H. Sun, Z.-Y. Ma, T. Ma, J. Xia, Y.-B. Zhu, R. Zhao, H.-B. Yao, H.-A. Wu, S.-H. Yu, *Matter* **2019**, *1*, 412-427.
[44] a) K. Wakabayashi, N. Sumi, S. Yamazaki, T. Uchida, K. Kimura, *Eur. Polym. J.* **2012**, *48*, 1787-1795; b) Z. Xu, X. Zhuang, C. Yang, J. Cao, Z. Yao, Y. Tang, J. Jiang, D. Wu, X. Feng, *Adv. Mater.* **2016**, *28*, 1981-1987; c) H. He, K. Rahimi, M. Zhong, A. Mourran, D. R. Luebke, H. B. Nulwala, M. Möller, K. Matyjaszewski, *Nat. Commun.* **2017**, *8*, 14057; d) S. J. Talley, S. L. Vivod, B. A. Nguyen, M. A. B. Meador, A. Radulescu, R. B. Moore, *ACS Appl. Mater. Interfaces* **2019**, *11*, 31508-31519.
[45] L. Jia, G. Guerin, Y. Lu, Q. Yu, I. Manners, M. A. Winnik, *Angew. Chem. Int. Ed.* **2018**, *57*, 17205-17210.
[46] Z. Geng, B. Xiong, L. Wang, K. Wang, M. Ren, L. Zhang, J. Zhu, Z. Yang, *Nat. Commun.* **2019**, *10*, 4090.
[47] a) H. Qiu, G. Russo, P. A. Rupar, L. Chabanne, M. A. Winnik, I. Manners, *Angewandte Chemie International Edition* **2012**, *51*, 11882-11885; b) A. M. Oliver, J. Gwyther, M. A. Winnik, I. Manners, *Macromolecules* **2018**, *51*, 222-231.
[48] a) J. Shao, I. A. B. Pijpers, S. Cao, D. S. Williams, X. Yan, J. Li, L. K. E. A. Abdelmohsen, J. C. M. van Hest, *Adv. Sci.* **2019**, *6*, 1801678; b) I. A. B. Pijpers, L. K. E. A. Abdelmohsen, D. S. Williams, J. C. M. van Hest, *ACS Macro Lett.* **2017**, *6*, 1217-1222.

[49] a) Y. Yang, J. Zhang, W. Zou, S. Wu, F. Wu, A. Xie, Z. Wei, *Macromol. Rapid Commun.* **2018**, *39*, 1700591; b) C. D. Vacogne, C. Wei, K. Tauer, H. Schlaad, *J. Am. Chem. Soc.* **2018**, *140*, 11387-11394.
[50] K. Liu, A. Levy, C. Liu, J.-H. Olivier, *Chemistry of Materials* **2018**, *30*, 2143-2150.
[51] Z. Wang, F. Liao, S. Yang, T. Guo, *Mater. Lett.* **2012**, *67*, 121-123.

Table of Content

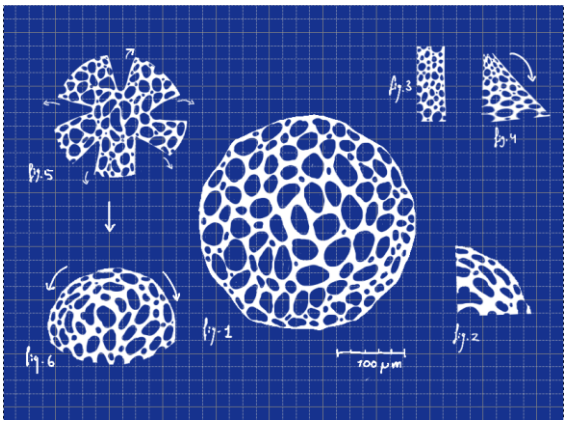

Biomorphic rendition: Nature has endowed extraordinary beauty and functional significance in the form of biological morphology. Aiming for expressing the nature in a synthetic manner, materials scientists and engineers have designed varieties of biomorphic superstructures from organic precursors.